
**Nanotechnologies — Characterization of
multiwall carbon nanotubes —
Mesoscopic shape factors**

*Nanotechnologies — Caractérisation des nanotubes en carbone
multicouches — Facteurs de forme mésoscopique*



Reference number
ISO/TS 11888:2011(E)

© ISO 2011



COPYRIGHT PROTECTED DOCUMENT

© ISO 2011

All rights reserved. Unless otherwise specified, no part of this publication may be reproduced or utilized in any form or by any means, electronic or mechanical, including photocopying and microfilm, without permission in writing from either ISO at the address below or ISO's member body in the country of the requester.

ISO copyright office
Case postale 56 • CH-1211 Geneva 20
Tel. + 41 22 749 01 11
Fax + 41 22 749 09 47
E-mail copyright@iso.org
Web www.iso.org

Published in Switzerland

Contents

Page

Foreword	iv
Introduction.....	v
1 Scope	1
2 Terms, definitions and abbreviations.....	1
2.1 Terms and definitions	1
2.2 Abbreviated terms	3
3 Sample preparation methods.....	3
3.1 Ball mill cutting.....	3
3.2 Dispersion method	3
3.3 Sample preparation for scanning electron microscope	3
4 Experimental procedure	4
4.1 Measurements of the SBPL using SEM	4
4.1.1 SEM	4
4.1.2 Measurement methods for the SBPL	4
4.2 Measuring inner and outer diameters of MWCNTs using TEM.....	5
5 Test report.....	5
Annex A (normative) Equations for terms and definitions in Clause 2 and Annexes B, C and D.....	6
Annex B (informative) Viscometry	10
Annex C (informative) Dynamic light scattering and depolarized dynamic light scattering.....	11
Annex D (informative) Case study and reports.....	13
Bibliography.....	17

Foreword

ISO (the International Organization for Standardization) is a worldwide federation of national standards bodies (ISO member bodies). The work of preparing International Standards is normally carried out through ISO technical committees. Each member body interested in a subject for which a technical committee has been established has the right to be represented on that committee. International organizations, governmental and non-governmental, in liaison with ISO, also take part in the work. ISO collaborates closely with the International Electrotechnical Commission (IEC) on all matters of electrotechnical standardization.

International Standards are drafted in accordance with the rules given in the ISO/IEC Directives, Part 2.

The main task of technical committees is to prepare International Standards. Draft International Standards adopted by the technical committees are circulated to the member bodies for voting. Publication as an International Standard requires approval by at least 75 % of the member bodies casting a vote.

In other circumstances, particularly when there is an urgent market requirement for such documents, a technical committee may decide to publish other types of document:

- an ISO Publicly Available Specification (ISO/PAS) represents an agreement between technical experts in an ISO working group and is accepted for publication if it is approved by more than 50 % of the members of the parent committee casting a vote;
- an ISO Technical Specification (ISO/TS) represents an agreement between the members of a technical committee and is accepted for publication if it is approved by 2/3 of the members of the committee casting a vote.

An ISO/PAS or ISO/TS is reviewed after three years in order to decide whether it will be confirmed for a further three years, revised to become an International Standard, or withdrawn. If the ISO/PAS or ISO/TS is confirmed, it is reviewed again after a further three years, at which time it must either be transformed into an International Standard or be withdrawn.

Attention is drawn to the possibility that some of the elements of this document may be the subject of patent rights. ISO shall not be held responsible for identifying any or all such patent rights.

ISO/TS 11888 was prepared by Technical Committee ISO/TC 229, *Nanotechnologies*.

Introduction

Multiwall carbon nanotubes (MWCNTs) synthesized by chemical vapor deposition (CVD) are of growing interest for use in polymer composites and conductive coatings. In many cases, MWCNTs synthesized by CVD have static (permanent) bend points randomly distributed along their axis. Physical and chemical properties of mass-produced MWCNTs are strongly dependent on the statistical distribution of mesoscopic shapes and sizes of the individual MWCNT (see ISO/TS 80004-3), among other parameters, that comprise the mass produced product (see References [3] to [5]). It is therefore crucial to characterize the mesoscopic shapes of MWCNTs in order to help ensure that the final properties are reproducible for use in a wide range of materials including composites and other dispersions, as well as for Environment, Health and Safety (EHS) issues^[6].

This Technical Specification provides methods for the characterization of mesoscopic shape factors of MWCNTs, including sample preparation procedures. In particular, it provides a statistical method for characterizing MWCNTs produced by the CVD method. During MWCNT synthesis, axial structures are not perfectly linear but include permanent bend points. This Technical Specification provides methods for determining a statistical quantity, representing a maximum straight length that is not deformed by permanent bending called the “static bending persistence length” (SBPL). The SBPL gives information regarding the relationship between the MWCNT mesoscopic shape and size. If two MWCNTs of equal length have different SBPL, their overall sizes (e.g. radius of gyration or an equivalent diameter such as a hydrodynamic diameter) will also be different from one another. In practical applications, the variation in SBPL affects both chemical reactivity and physical properties^{[3][4][5]}.

Electrical conductivity and dimensional stability of MWCNT-polymer compounds are also strongly dependent on the SBPL of the MWCNT used to make them^{[3][4][5]}. Various properties might be affected by SBPL, including electrical percolation threshold^{[5][7]}, toxicity^[6], thermal conductivity^[8], rheological property^[9], and field emission property^[10]. SBPL could be useful for estimating the loading of a polymer CNT matrix to achieve electrical conductivity (percolation limit) and should also assist with modelling the mechanical properties of polymer-CNT composites with different loadings.

Prior to commencing any work, readers are advised to familiarise themselves with the latest guidance on handling and disposal of MWCNTs, particularly in relation to the use of appropriate personal protective equipment. Information on current practices is available in ISO/TR 12885.

Nanotechnologies — Characterization of multiwall carbon nanotubes — Mesoscopic shape factors

1 Scope

This Technical Specification describes methods for the characterization of mesoscopic shape factors of multiwall carbon nanotubes (MWCNTs). Techniques employed include scanning electron microscopy (SEM), transmission electron microscopy (TEM), viscometry, and light scattering analysis.

This Technical Specification also includes additional terms needed to define the characterization of scattered bending persistence length (SBPL). Two approximation methods are given for the evaluation of SBPL (which generally varies from several tens of nanometers to several hundred micrometers).

Well-established concepts and mathematical expressions, analogous to polymer physics, are utilized for the definition of mesoscopic shape factors of MWCNTs.

2 Terms, definitions and abbreviations

2.1 Terms and definitions

For the purposes of this document, the following terms and definitions apply.

NOTE Equations for terms and definitions are given in Annex A.

2.1.1

mesoscopic shape

description of shape at the observation scale for an individual multiwall carbon nanotube (MWCNT)

NOTE 1 Mesoscopic shape factors describe the average size and shape of individual MWCNTs, while “macroscopic” describes the shape and size of MWCNT aggregates or agglomerates. “Atomic scale resolution” describes the shape of an MWCNT at the atomic level (see Figure 1).

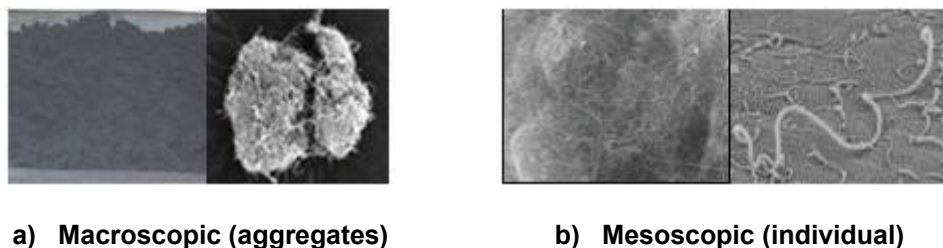
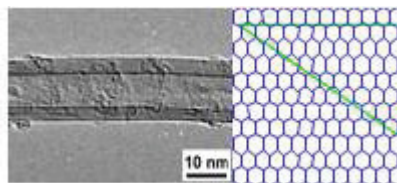


Figure 1 — Shape of MWCNTs at various scales (*continued*)



c) Atomic scale resolution

NOTE 2 See Reference [3].

NOTE 3 Copyright (c) 2010 ACS.

Figure 1 — Shape of MWCNTs at various scales

2.1.2

regular shape

⟨MWCNTs⟩ property of having regular pattern along tube axis

NOTE Correlations in the direction of the tangent show a periodical shape for MWCNTs of regular shape. Both straight and coil-shaped MWCNTs are typically classified as MWCNTs of regular shape.

2.1.3

random shape

⟨MWCNTs⟩ property of having static, or permanent, bend points distributed randomly (Gaussian) along their axis

2.1.4

SBPL

static bending persistence length

l_{sp}

maximum straight length without static bending

2.1.5

contour length

L

total length of an MWCNT along its axis

2.1.6

weighted average contour length

\bar{L}_w

average of contour length which is assigned a weight

2.1.7

end-to-end distance

R

straight distance between the two ends of an MWCNT

2.1.8

bending ratio

D_b

ratio between mean-squared end-to-end distance and squared contour length

2.1.9

intrinsic viscosity

$[\eta]$

description of an MWCNT's contribution to the viscosity of MWCNT dispersion

2.2 Abbreviated terms

CVD	chemical vapor deposition
DDLS	depolarized dynamic light scattering
DLS	dynamic light scattering
DMF	dimethylformamide
SEM	scanning electron microscope
SBPL	static bending persistence length
TEM	transmission electron microscopy

3 Sample preparation methods

3.1 Ball mill cutting

Place 200 mg of MWCNTs and 20 ml of ethanol and zirconia balls into a zirconia pot (150 ml) and ball-mill 500 r/min for 2 h.

Pour the ball-milled MWCNT dispersion from the zirconia pot into a 50 ml conical centrifuge tube at 5 000 r/min.

Centrifuge the ball-milled MWCNT dispersion to separate the MWCNTs and then freeze-dry the separated MWCNTs for 24 h. Dry the MWCNTs at 300 °C for 30 min while exposed to air to remove unwanted volatile components.

Grind the dried MWCNTs by pestle and mortar.

NOTE When higher r/min and longer ball-milling time is applied than those described here, the structure of MWCNTs might be destroyed.

3.2 Dispersion method

Disperse 0,02 g of milled MWCNTs in 200 ml dimethylformamide (DMF) using an ultra-sonicator at 40 W for 3 h. Pour the MWCNT dispersion into a 50 ml conical centrifuge tube and centrifuge at 3 000 r/min for 30 min. Filter the dispersion with a paper filter to eliminate any non-dispersed parts that might remain.

NOTE DMF is the best solvent for CNT dispersion (see Reference [3]).

3.3 Sample preparation for scanning electron microscope

Use additional DMF to dilute the MWCNT dispersion to 10x. Drop 1 ml of the 10x dispersion onto a 0,02 µm ceramic filter and filter it under vacuum. Dry the ceramic filter, containing the MWCNTs, at 60 °C for 24 h.

NOTE This procedure is recommended for Method 1 (see 4.1.2.1) and Method 3 (see 4.1.2.3). As-synthesized MWCNTs can be used for Method 2 (see 4.1.2.2).

4 Experimental procedure

4.1 Measurements of the SBPL using SEM

4.1.1 SEM

4.1.1.1 General

High resolution SEM images allow closely spaced features to be examined at a high magnification.

4.1.1.2 Preparing SEM images

Cut the ceramic filter containing the MWCNTs into small pieces and place on a sample holder, to which conductive tape is applied. Dry the sample holder under vacuum at 40 °C for 1 h. Sputter coat the dried sample with iridium for 1 min. Gold or platinum may be used if an iridium source is not available. Take three or more SEM images at a magnification of 10 000x. Take three or more representative high resolution images at 20 000x.

NOTE 1 This procedure is recommended for Method 1 (4.1.2.1) and Method 3 (4.1.2.3).

Alternatively, place an as-synthesized MWCNT on a sample holder, to which conductive tape is applied. Dry the sample holder under vacuum at 40 °C for 1 h. Sputter coat the dried sample with iridium for 1 min. Gold or platinum may be used if an iridium source is not available. Take three or more SEM images at a magnification of 10 000x. Take three or more representative high resolution images at 20 000x.

NOTE 2 This procedure is recommended for Method 2 (see 4.1.2.2).

4.1.2 Measurement methods for the SBPL

4.1.2.1 Method 1

From the SEM images, determine the contour lengths and end-to-end distances of at least 100 different individual MWCNTs. Classify the data using an interval of 100 nm for contour length. For each contour length range, calculate mean-squared end-to-end distance.

Obtain the bending ratio for each contour length range by dividing the mean-squared end-to-end distance by squared average contour length [see Equation (A.3)]. When the contour length is greater than 1 μm , the value of contour length from the top view image may be underestimated by up to 15 %^[3]. When more accurate values are required, measure the contour length and end-to-end distance using a 3-D image, which can be obtained by several side view images^[3].

Plot the bending ratio with respect to the reciprocal contour length, measure the gradient and determine the SBPL using Equation (A.4). When the linear relationship between bending ratio and reciprocal contour length reaches the asymptotic limit, the resulting slope equals 2 times the SBPL.

NOTE 1 For MWCNTs of random shape, the end-to-end distance varies at constant contour length^[3]. Therefore, various values of end-to-end distance could be measured for each contour length range. The distribution of end-to-end distance of MWCNT is Gaussian for each contour length range when MWCNT are in random shape. To obtain the mean-squared end-to-end distance, calculate the mean value of the squared end-to-end distance.

NOTE 2 Because well-dispersed MWCNTs are filtered prior to SEM imaging, 100 MWCNTs are sufficiently representative of the shape of the MWCNTs in the sample. This is supported by dynamic light scattering (DLS) and depolarized dynamic light scattering (DDLS) measurements as well as intrinsic viscosity measurements^[3]. An approximate value for the SBPL can be obtained using Method 2 or Method 3.

4.1.2.2 Method 2

Measure the radius of curvature of at least 100 individual tubes from the SEM images of as-synthesized MWCNTs, then calculate the mean value of the radius of curvature. This mean radius is approximately equal to the value of SBPL.

4.1.2.3 Method 3

From the SEM image, select at least 10 MWCNTs with a contour length in the range of $2,0 \pm 0,2 \mu m$. Measure the end-to-end distance of each MWCNT. The approximate value for SBPL can be obtained from the mean-squared end-to-end distance and the squared average contour length [see Equations (A.3) and (A.4)].

NOTE 1 Method 1 is the most accurate method but it is time consuming. The SBPL estimated by Method 2 has up to 20 % deviation compared to Method 1 (Method 2 has a tendency to underestimate the SBPL). The SBPL estimated by method 3 has up to 100 % deviation compared to the value obtained by Method 1. The order of magnitude of SBPL has consequences for many applications such as transparent conductive film, electrode and polymer composites.

NOTE 2 The values of SBPL obtained by Methods 1, 2, and 3 can be confirmed by the viscometry method (Annex B) and/or the light scattering method (Annex C).

4.2 Measuring inner and outer diameters of MWCNTs using TEM

Place a droplet of the diluted, MWCNT/DMF dispersion onto a carbon-coated copper grid. Dry the grid at 60 °C for 24 h. Take TEM images at 10 000x magnification. Take three or more high resolution images at 1 000 000x to 3 000 000x of the MWCNT.

In order to obtain averages, measure the inner and outer diameters at not less than three different positions along the axis for at least 10 different MWCNTs. At least 30 total measurements are required.

5 Test report

The test report shall contain the following information (see Annex D):

- a) a full description of the sample preparation method(s) used;
- b) average inner and outer diameter;
- c) method used to determine SBPL;
- d) SBPL;
- e) all information necessary for evaluating the SBPL.

The test report may also include information relating to weighted average contour length and bending ratio (optional).

Annex A (normative)

Equations for terms and definitions in Clause 2 and Annexes B, C and D

A.1 Equations for terms and definitions in Clause 2

A.1.1

SBPL

static bending persistence length

 l_{sp}

maximum straight length without static bending

The overall size of MWCNTs of random shape scale with the square root of its contour length, L , as expressed by Equation (A.1) for the case $L \gg l_{sp}$ [3].

$$\langle R^2 \rangle = 2l_{sp}L + 2l_{sp}(e^{-L/l_{sp}} - 1) \quad (A.1)$$

l_{sp} is SBPL. The following terms apply to MWCNTs of random shape.

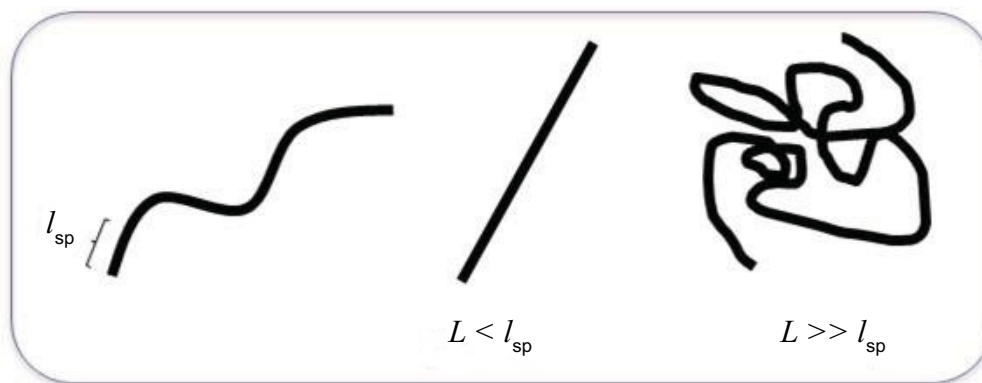


Figure A.1 — SBPL of an MWCNT

A.1.2

bending ratio

 D_b

ratio between mean-squared end-to-end distance and squared contour length

The bending ratio, D_b , is determined by the number of static bend points and their distribution along the MWCNT axis. D_b is expressed as in Equation (A.2) [3].

$$D_b \equiv \frac{\langle R^2 \rangle}{L^2} \cong \sum_{i=1}^k \varphi_i^2 \quad (A.2)$$

where $\varphi_i = N_i / N$ (each segment, i , consists of N_i unit segments);

N is the total number of unit segments in an MWCNT;

N_i is the number of unit segments in the i -direction segments;

$k = m + 1$, where m is the number of static bend points;

$\langle R^2 \rangle$ is mean-squared end-to-end distance;

L is contour length.

SBPL is defined by Equation (A.3)^[3]. Using SBPL is more convenient than using bending ratio because the former does not depend on contour length as it is obtained in an asymptotic limit^[3]. $2l_{sp}$ can be obtained from the slope when D_b is plotted versus $1/L$. When contour length is long enough, $1/L$ approaches zero.

$$D_b \equiv \frac{\langle R^2 \rangle}{L^2} \equiv \left(\frac{2l_{p0}}{L} \right) \left(\frac{1 + \cos(\theta)}{1 - \cos(\theta)} \right) = C \left(\frac{2l_{p0}}{L} \right) = \frac{2l_{sp}}{L} \quad (A.3)$$

where

C is a constant;

θ is a static bent angle between the direction of $(i+1)^{th}$ segment and the axis direction of i^{th} segment when i^{th} segment and $(i+1)^{th}$ segment is a neighbour; θ is 90° ;

l_{p0} is a segment length, assuming all segments in an MWCNT have equal length.

A.1.3

weighted average contour length

\bar{L}_w

average of contour length which is assigned a weight

NOTE Weighted average contour length, \bar{L}_w , is used for evaluating SBPL in SEM, DLS, and viscometry analysis.

$$\bar{L}_w \equiv \frac{\sum_{i=1}^N N_i L_i^2}{\sum_{i=1}^N N_i L_i} \quad (A.4)$$

where

N is the total number of individual MWCNT nano-objects;

N_i is the number of MWCNT having a length of L_i .

Weighted average end-to-end distance, \bar{R}_w , can be obtained by combining Equations (A.2) and (A.4), which is used for the estimation of intrinsic viscosity in Annex B.

A.1.4

intrinsic viscosity

$[\eta]$

description of an MWCNT's contribution to the viscosity of MWCNT dispersion

Intrinsic viscosity, $[\eta]$, is defined by Equations (A.5), (A.6), and (A.7)^[3].

$$[\eta] = 2,20 \times 10^{21} \frac{f}{M_{aw}} \left\langle \overline{R_w^2} \right\rangle^{3/2} \quad (A.5)$$

$$f = \left[1 + 0,926 \Delta (D_b)^{1/2} \right]^{-1} \quad (A.6)$$

$$\Delta = \ln \left(\frac{2l_{sp}}{D_o} \right) - 2,431 \quad (A.7)$$

A.2 Equations for other terms and definitions

A.2.1

dynamic bending persistence length

l_p

maximum straight length that is not bent by thermal energy

Where MWCNTs are dispersed, the value for dynamic bending persistence length depends on the type of solvent used. The Kratky-Porod expression for l_p is given in Equation (A.8).

$$\left\langle R^2 \right\rangle = 2l_p L + 2l_p (e^{-L/l_p} - 1) \quad (A.8)$$

where

$\left\langle R^2 \right\rangle$ is mean-squared end-to-end distance, which is the mean value of squared end-to-end distance;

L is contour length, which is the total length of an MWCNT along its axis.

A.2.2

apparent persistence length

l_{ap}

measured value of persistence length of an MWCNT by dynamic light scattering

When an MWCNT in a dispersion is exposed to thermal energy, its overall size and shape changes. The apparent persistence length, l_{ap} , is determined by the contributions of SBPL, l_{sp} , static bent angle, θ , and dynamic bent angle, $\Delta\theta$, according to Equation (A.9).

l_{ap} can be measured by DLS (see Annex C).

$$l_{ap} = l_{sp} \left(\frac{1 + \cos(\theta + \Delta\theta)}{1 - \cos(\theta + \Delta\theta)} \right) \left(\frac{1 - \cos(\theta)}{1 + \cos(\theta)} \right) \quad (A.9)$$

The dynamic bent angle is the change of bent angle by thermal energy. The dynamic bent angle is usually less than 2° at moderate temperatures, so apparent persistence length can be approximated by the SBPL.

A.2.3

apparent molecular weight

M_a

description of the molecular weight of an MWCNT, assuming the individual MWCNT is a molecule

Apparent molecular weight, M_a , is defined by Equation (A.10):

$$M_a = \rho N_{\text{avo}} \left(\frac{\pi (\bar{D}_O^2 - \bar{D}_I^2) L}{4} \right) \quad (\text{A.10})$$

where

ρ is the density of graphene layers of an individual MWCNT;

N_{avo} is Avogadro's number;

\bar{D}_O is the average outer diameter of an MWCNT;

\bar{D}_I is the average inner diameter of an MWCNT.

A.2.4 weighted average apparent molecular weight

\bar{M}_{aw}
average of apparent molecular weight which is assigned a weight

The weighted average apparent molecular weight, \bar{M}_{aw} , is defined by Equation (A.11):

$$\bar{M}_{\text{aw}} = \frac{\sum_{i=1}^N N_i M_{\text{ai}}^2}{\sum_{i=1}^N N_i M_{\text{ai}}} \quad (\text{A.11})$$

where

N is the total number of individual MWCNTs;

N_i is the number of MWCNTs having apparent molecular weight, M_{ai} ;

\bar{M}_{aw} is used for the estimation of intrinsic viscosity in Annex B.

A.2.5 relative viscosity

η_r
ratio of the viscosity of a dispersion to the viscosity of the solvent used

Relative viscosity, η_r , can be estimated by the ratio between the time during which MWCNT dispersion passes the viscometer capillary, t_{MWCNT} , and the time during which pure DMF containing no MWCNT passes the viscometer capillary, t_{DMF} .

$$\eta_r = \frac{t_{\text{MWCNT}}}{t_{\text{DMF}}} \quad (\text{A.12})$$

A.2.6 specific viscosity

η_s
ratio of the [viscosity](#) of a [dispersion](#) to the viscosity of the [solvent](#) used minus one

Specific viscosity, η_s , can be obtained from relative viscosity using Equation (A.13):

$$\eta_s = \eta_r - 1 \quad (\text{A.13})$$

Annex B (informative)

Viscometry

B.1 General

Intrinsic viscosity of MWCNT dispersion can be estimated by weighted average apparent molecular weight, \overline{M}_{aw} , weighted average contour length, \overline{L}_w , and SBPL, l_{sp} . If there are known values of \overline{M}_{aw} and \overline{L}_w , l_{sp} can be estimated from the measured value of intrinsic viscosity. The viscometry method confirms the SBPL values obtained by measurement methods in 4.1.2.

B.2 Mesoscopic shape factor from intrinsic viscosity measurement

Clean the viscometer with DMF three times.

Using a viscometer with a capillary diameter of 0,46 mm is recommended because the resolution is inadequate for larger diameters and MWCNT aggregation can occur for smaller diameters.

Measure the time during which pure DMF containing no MWCNTs passes the viscometer capillary. Using additional DMF, dilute the MWCNT dispersion (prepared in accordance with 3.2) to 0,001 to 0,005 wt.%. Pour the diluted MWCNT dispersion into the viscometer. Measure the time during which 0,001 to 0,005 wt.% MWCNT dispersion passes the viscometer capillary.

Calculate the relative and specific viscosities of the MWCNT dispersion using Equations (A.12) and (A.13) in Annex A. Divide the specific viscosity by the MWCNT concentration. Plot the quotient with respect to the MWCNT concentration. Determine intrinsic viscosity by extrapolating the quotient to zero MWCNT concentration.

The value obtained for the intrinsic viscosity of the MWCNT dispersion can be used to estimate the SBPL by use of Equations (A.5), (A.6), and (A.7) in Annex A, provided that values for the weighted averaged apparent molecular weight and weighted averaged end-to-end distance are known.

Annex C (informative)

Dynamic light scattering and depolarized dynamic light scattering

C.1 General

Translational and rotational diffusion coefficients of MWCNTs can be measured by dynamic light scattering (DLS) and depolarized dynamic light scattering (DDLS). The diffusion coefficients can be estimated by apparent persistence length, l_{ap} , average outer diameter of MWCNT, $\overline{D_O}$, and weighted average contour length, $\overline{L_w}$. The light scattering method confirms the SBPL values obtained by measurement methods in 4.1.2.

C.2 Mesoscopic shape factor from light scattering measurement

DLS and DDLS are used to measure the translational and the rotational diffusion of MWCNTs. Using a Diode-Pumped Solid State Laser (DPSSL), supply approximately 100 mW at $\lambda_0 = 532$ nm.

NOTE Using higher power can result in an undesirable temperature increase of the MWCNT.

Use a 256-channel digital autocorrelator with a 480 ns minimum delay time to compute the scattered photons time autocorrelation function.

Measure the autocorrelation function at several scattering angles ranging between 30° to 90°. Apply the polarizer and the detector, each having 1:100 000 extinction ratio to the DLS. Rotate the detector with 1° resolution using the motor control unit.

The DLS cell should be controllable to 1 K above a temperature range between 278 K to 393 K. Translational and rotational diffusion coefficients can be obtained from the first cumulant of the average decay rate, Γ , of the electric field autocorrelation. When incident light and detector are both vertically oriented, the translational diffusion coefficient is obtained from the slope of the curve plotted for the average decay rate with respect to the square scattering vector magnitude:

$$q = 4\pi n \sin(\theta_s / 2) / \lambda_0$$

where

n is dispersion refractive index;

θ_s is scattering angle;

λ_0 is incident light wavelength *in vacuo*.

In order to avoid a hydrodynamic interaction effect, a very dilute dispersion of $n_M L^3 = 0,5$ is recommended for DLS measurement, where n_M is the number of MWCNTs. Measure the first cumulant of the average decay rate, Γ , of the electric field autocorrelation function. When the incident light and detector are both vertical, Γ is expressed as Γ_{VV} . The translational diffusion coefficient, D_T , is characterized by Equation (C.1)^[11].

$$\Gamma_{VV} = q^2 D_T \tag{C.1}$$

When the incident light is vertical and the detector is horizontal, Γ is expressed as Γ_{Hv} . The translational diffusion coefficient and rotational diffusion coefficient, D_R , is characterized by Equation (C.2)^[11].

$$\Gamma_{Hv} = q^2 D_T + 6 D_R \quad (C.2)$$

There are three unknown factors for shape and size of MWCNTs: average diameter, SBPL and weighted average contour length. With the average diameter data obtained by an independent method, SBPL and weighted average contour length can be evaluated by comparing Equation (C.3) and Equation (C.4) to experimental data^[4]. In Annex D, experimental data are compared to the calculation data.

$$D_T = \frac{kT}{3\pi\eta_s \bar{L}_w} \left[1 + \ln(2L_{ap}) - 2,431 + 1,843 \left(N / 2L_{ap} \right)^{1/2} + 0,138 \left(N / 2L_{ap} \right)^{-1/2} - 0,305 \left(N / 2L_{ap} \right)^{-1} \right] \quad (C.3)$$

$$L_{ap} = l_{ap} / \bar{D}_O \quad \text{and} \quad N = \bar{L}_w / \bar{D}_O$$

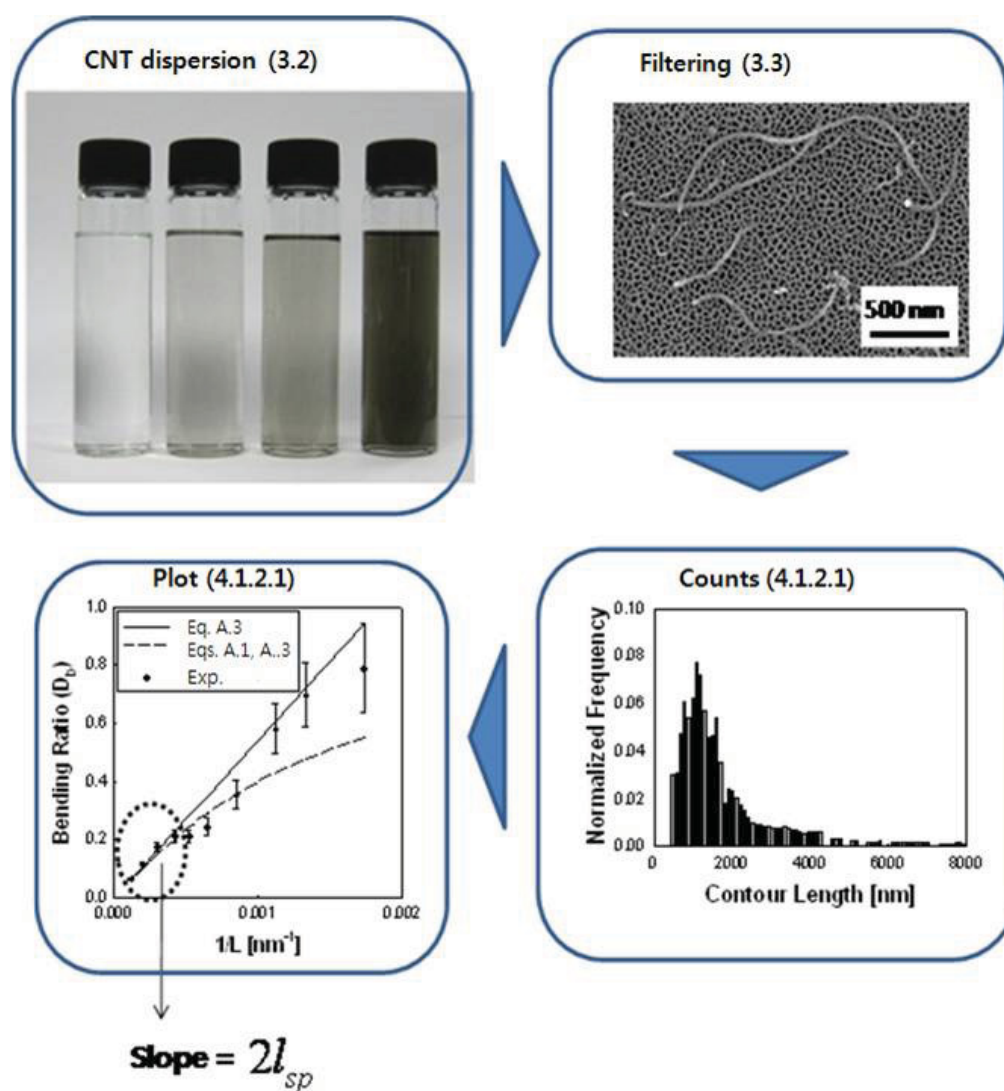
$$D_R = \left(\frac{kT}{\eta_s} \right) \left(\frac{2}{l_{ap} \bar{L}_w^2} \right) \left[0,253 \left(\frac{\bar{L}_w}{4l_{ap}} \right)^{1/2} + 0,59 \ln(2L_{ap}) - 0,227 \right] \quad (C.4)$$

SBPL measured by DLS represents the average shape of MWCNTs in a dispersion.

Annex D (informative)

Case study and reports

A brief summary for the measurement of SBPL using Method 1 is illustrated in Figure D.1.



NOTE 1 Copyright (c) 2010 ACS.

NOTE 2 Images sourced from Reference [3].

Figure D.1 — Pictorial process flow for the measurement of SBPL using Method 1

Mesoscopic shape factors of various MWCNTs can be reported as shown in Table D.1. In the report of mesoscopic shape factors, it is recommended that the average outer diameter and SBPL, l_{sp} , be included. The measurement method for evaluating l_{sp} should be reported. Contour length and bending ratio can optionally be included in the report. Because the order of magnitude of l_{sp} has physical significance, it is recommended that the values of l_{sp} are expressed, e.g. $A \times 10^B$, where A and B are integers.

Table D.1 — Example of the report of mesoscopic shape factors

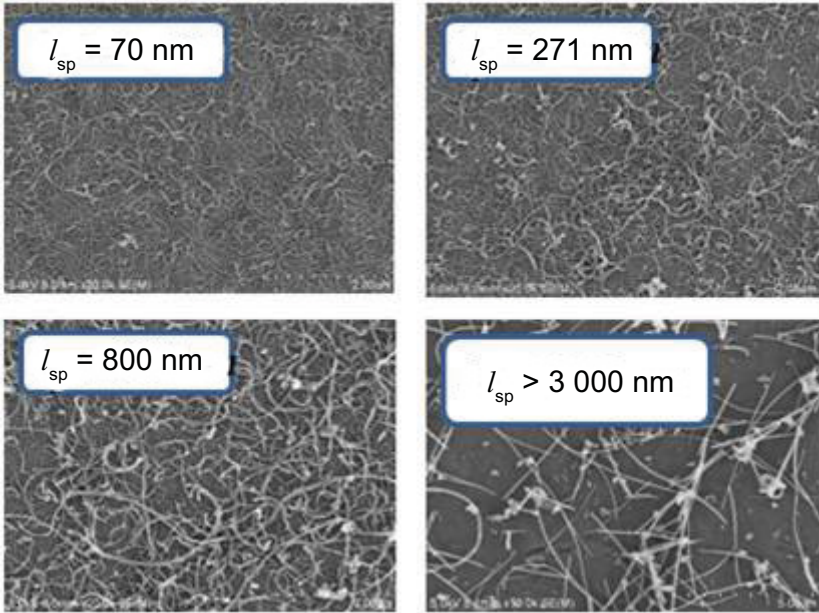
	MWCNT 1	MWCNT 2	MWCNT 3	MWCNT 4
Average outer diameter nm ^a	9,5	21	35	50
l_{sp} by Method 1 nm	7×101	3×102	8×102	$>3 \times 103$
l_{sp} by Method 2 nm	6×101	2×102	7×102	$>3 \times 103$
l_{sp} by Method 3 nm	$7 \times 101 \sim 12 \times 101$	$2 \times 102 \sim 3 \times 102$	$7 \times 102 \sim 1 \times 103$	$>3 \times 103$
Contour length \bar{L}_w ^b	1 416	1 718	2 045	2 035
Bending ratio, D_b	0,09	0,28	0,50	1,00

^a Arithmetic average.

^b According to Equation (A.4).

SEM images for various MWCNTs are shown in Figure D.2.

Figure D.2 also shows that more tortuous shaped MWCNTs have shorter SBPL.



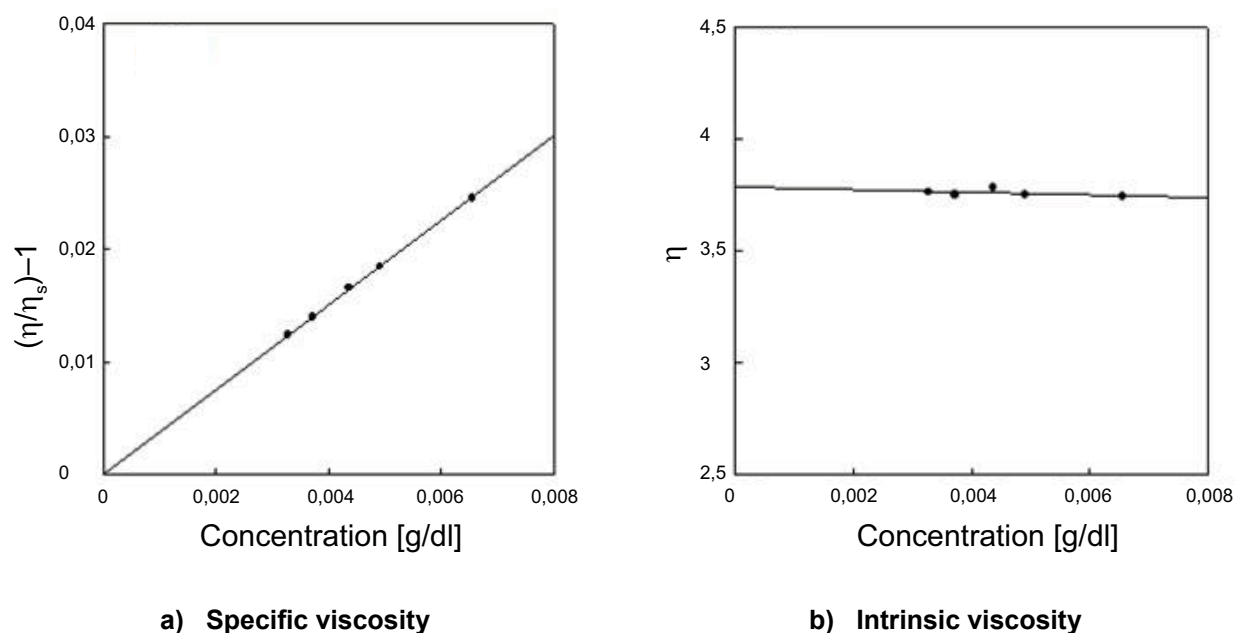
NOTE The shapes of the MWCNTs have been well characterized by SBPL.

Figure D.2 — SEM images of various MWCNTs

In this annex, the intrinsic viscosity calculated by Equation (C.1), using the mesoscopic shape factors as reported in Table D.1, is compared to the experimentally measured intrinsic viscosity. Intrinsic viscosity is obtained from the experimental data using Equation (D.1) as shown in Figure D.3.

$$[\eta] = \lim_{C \rightarrow 0} \frac{(\eta / \eta_s) - 1}{C} \quad (D.1)$$

The solid line in Figure D.3 indicates the calculated results using Equation (C.1) with the mesoscopic shape factors shown in Table D.1. The measured intrinsic viscosity for MWCNT is consistent with the calculated results. This result indicates that the methods in Clause 4 are correct.



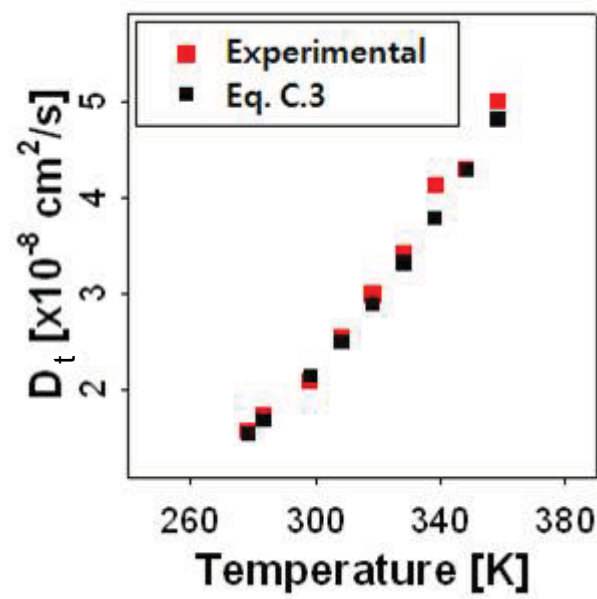
NOTE 1 Copyright (c) 2010 ACS.

NOTE 2 See Reference [3].

Figure D.3 — Specific viscosity and intrinsic viscosity of MWCNT dispersions

Figure D.4 shows that the translational diffusion coefficient of MWCNT dispersion is coincident with the value calculated using Equation (C.3) with the mesoscopic shape factors.

This study also shows overall size (end-to-end) distance of MWCNT is decreased with the increase of temperature, which is ascribed to thermal fluctuation at static bend points. Neglecting the thermal fluctuation effect, the average size of MWCNT evaluated from DLS measurement is consistent with the size from SEM images (Method 1 in 4.1.2.1) within 20 % error for the entire temperature range in Figure D.4. This result validates the methods presented in Clause 4.



NOTE 1 Copyright (c) 2010 ACS.

NOTE 2 See Reference [4].

Figure D.4 — Translational diffusion coefficient of MWCNT dispersion at various temperatures

Bibliography

- [1] ISO/TR 12885, *Nanotechnologies — Health and safety practices in occupational settings relevant to nanotechnologies*
- [2] ISO/TS 80004-3, *Nanotechnologies — Vocabulary — Part 3: Carbon nano-objects*
- [3] LEE, H.S., YUN, C.H., KIM, H.M., LEE, C.J., "Persistence Length of Multiwalled Carbon Nanotubes with Static Bending," *J. Phys. Chem. C* 111, 18882-18887 (2007)
- [4] LEE, H.S., YUN, C.H., "Translational and Rotational Diffusions of Multiwalled Carbon Nanotubes with Static Bending," *J. Phys. Chem. C* 112, 10653-10658 (2008)
- [5] LEE, H.S., YUN, C.H., KIM, S.K., CHOI, J.H., LEE, C.J., JIN, H.J., LEE, H., PARK, S.J., PARK, M., "Percolation of Two-dimensional Multiwall Carbon Nanotube Networks," *Appl. Phys. Lett.*, 95, 134104 (2009)
- [6] POLAND, C.A., DUFFIN, R., KINLOCH, I., MAYNARD, A., WALLACE, W.A.H., SEATON, A., STONE, V., BROWN, S., MACNEE, W., DONALDSON, K., "Carbon Nanotubes Introduced into the Abdominal Cavity of Mice Show Asbestoslike Pathogenicity in a Pilot Study," *Nature Nanotechnology*, 3, 423, (2008)
- [7] POORTEMAN, M., TRAIANIDIS, M., BISTER, G., CAMBIER, F., "Colloidal Processing, Hot Pressing and Characterization of Electroconductive MWCNT-alumina Composites with Compositions near the Percolation Threshold," *J. Eur. Cer. Soc.*, 29, 669 (2009)
- [8] DENG and XZHENG, "Interactio Models for Effective Thermal and Electric Conductivities of Carbon Nanotube Composites," *Acta Mechania Solida Sincia*, 22, No1, (2009)
- [9] HOBBIIE, E.K., "Shear Rheology of Carbon Nanotube Suspensions," *Rheol acta*, 49, 323 (2010)
- [10] JANG, H.S., LEE, H.-R., KIM, D.-H., "Field Emission Properties of Carbon Nanotubes with Different Morphologies," *Thin Solid Films*, 500, 124 (2006)
- [11] BERNE, B., PECORA, R., *Dynamic Light Scattering*, Wiley, New York, 1976, Chapter 8

